Interaction between a tubular beam of charged particles and a dispersive metamaterial of cylindrical configuration

Yu. O. Averkov,* Yu. V. Prokopenko,† and V. M. Yakovenko‡

A. Ya. Usikov Institute for Radiophysics and Electronics, National Academy of Sciences of Ukraine, 12 Academician Proskura Street, 61085 Kharkov, Ukraine

(Received 18 April 2017; published 10 July 2017)

The interaction between a tubular beam of charged particles and a dispersive metamaterial of cylindrical configuration has been investigated theoretically. This metamaterial may have negative permittivity and negative permeability simultaneously over a certain frequency range where it behaves like a left-handed metamaterial. The dispersion equation for the eigenmodes spectra of a metamaterial and the coupled modes spectra of the system have been derived and numerically analyzed. It has been found that the absolute beam instability of bulk-surface waves occurs because of peculiarities of the eigenmodes spectra of a left-handed metamaterial. Specifically, the resonant frequency behavior of the permeability causes the emergence of the sections of dispersion curves with anomalous dispersion. It has been demonstrated that the symmetric bulk-surface mode with two field variations along the cylinder radius possesses the maximum value of instability increment. The obtained results allow us to propose the left-handed metamaterial as the delaying medium in oscillators of electromagnetic radiation without a need to provide an additional feedback in the system just as in a backward-wave tube.

DOI: 10.1103/PhysRevE.96.013205

I. INTRODUCTION

Since the traveling-wave amplifier was created by Kompfner (see Ref. [1]) in the 1940s, there have been many theoretical and experimental works devoted to transforming a kinetic energy of charged particle flows into an electromagnetic radiation (see, e.g., Refs [2–6] and the references cited therein). At the present time, there is a tendency toward the advancement in millimeter and submillimeter wavelength ranges in the development of electron-vacuum technology. At the same time, the use of traditional approaches to electronic device design is experiencing great difficulties due to the small geometric dimensions of the main elements. There is a need to use oversized (with respect to the wavelength of generated oscillations) electrodynamic structures operating in a multimode regime. The stability of the generation frequency requires excitation and selection of a high-order working mode in such structures. The possibility of excitation of the weakly decaying high-order modes (so-called "whispering gallery" modes) in cylindrical dielectric resonators (CDRs) predetermines their use in the vacuum electronic devices of the short-wave range of millimeter and submillimeter wavelengths. Then, the above-mentioned structural difficulty is overcome. However, the output power of traditional sources drops down sharply with a transition to submillimeter wavelengths [7]. Hence it becomes necessary to use high-energy oscillators excited by electron flows. It is important to note in this connection that with powerful new technologies many types of artificial materials can be fabricated which are endowed with unique electromagnetic properties and show promise as structural elements for the high-energy oscillators. For instance, among them there are the metal-based (see, e.g., Refs. [8–15]), all-dielectric [16], and graphene-based [17] metamaterials which behave like left-handed ones over a certain frequency range. Below we dwell on electromagnetic properties of left-handed metamaterials (LHMs) in more detail.

In [18], the results of investigations of an auto-oscillatory system based on a high-quality CDR with whispering gallery modes excited by the azimuthal-periodic current of a relativistic electron beam were presented. The possibility of using the investigated system or its modifications is shown in the millimeter wavelength range. The appearance of the detected electromagnetic radiation is associated with the excitation of CDR whispering gallery modes by a disturbed flow of charged particles. The theoretical description of the phenomena that lead to the appearance of the radiation found in Ref. [18] is rather a difficult problem. Therefore, from our viewpoint, it seems appropriate to use the simplified physical models of the electrodynamic system discussed in Ref. [18], which allow qualitative and quantitative descriptions of physical phenomena that are as close as possible to the experimental conditions. The simplest physical model is a radially thin tubular electron beam moving along an infinitely long solid-state cylinder.

An actual problem of radiophysics and electronics is the investigation of the generation mechanisms of electromagnetic waves that are excited when charged particles move in various electrodynamic systems. To create sources of electromagnetic radiation in the millimeter and submillimeter ranges, the beam instabilities occurring in electrodynamic systems of various kinds are of great interest. Particular attention is given to multiwave Cherenkov generators of surface waves [19,20] and auto-oscillatory systems based on dielectric resonators [18,21,22]. The energy loss of one particle per unit time for eigenmode excitation in systems is one of the fundamentally important characteristics of the possible generation process [23–30]. Besides, the beam instabilities that occur in electrodynamic systems containing dispersive media are of special interest. In particular, the instability of

*yuriyaverkov@gmail.com
†prokopen@ire.kharkov.ua
‡yavm@ire.kharkov.ua

the tubular electron beam that interacts with a plasmalike medium was studied in Ref. [31]. In addition, an actual problem is the investigation of the electromagnetic properties of solid-state structures containing left-handed media. The technology progress of fabricating metamaterial structures stimulates studying the excitation mechanisms of their eigenmodes.

Indeed, in recent years a good deal of attention has been given to studying the electromagnetic properties of the left-handed media. We recall that these materials came to be known by this particular name because in these media the directions of electric and magnetic field vectors as well as the direction of a wave vector form a left-handed triplet. The unusual properties of the left-handed medium (LHM) electrodynamics were originally suggested in Refs. [32,33]. The authors of Ref. [32] first proved the possibility of excitation of the electromagnetic waves with negative group velocity with the aid of Cherenkov radiation in a medium, which possesses negative permittivity ε and negative permeability μ simultaneously. In addition to that it was shown that if an electron moves from vacuum into the medium, the maximum of the intensity of Cherenkov radiation is in vacuum and the Cherenkov angle in this case is obtuse. The unusual properties of the LHM electrodynamics were originally classified in Ref. [33], where it was demonstrated that the LHM would exhibit unusual properties such as the negative index of refraction, antiparallel wave vector **k** and Poynting vector **S**, antiparallel phase and group velocities, and the time-averaged energy flux opposite to the time-averaged momentum density. Besides, as indicated in Ref. [33], opposite directions of vectors **S** and **k** in the LHM result in a reverse Doppler shift and the other phenomena of interest.

LHMs have evoked considerable interest since they were practically implemented in Refs. [8–12] in the form of alternating layers with negative ε and positive μ and the layers with positive ε and negative μ. The permeability frequency dispersion of complex composites is provided by a periodic structure of nonmagnetic circular conducting units such as the split ring resonators, spirals, etc. The permittivity frequency dispersion is provided by a periodic grating of thin conducting wires. If a wavelength of the electromagnetic wave that propagates in such a material is much greater than the period of composite structure, the composite for this particular wave is similar to a continuous one. In Refs. [8–12] the parameters of structural elements are selected in such a way that ε and μ become negative over the GHz frequency range. Since then, a large variety of metal-based and all-dielectric LHMs with different types of unit-cell geometries has been proposed (see, e.g., Refs. [13–16]). For instance, in Ref. [15] the silver-based unit cells were fabricated on a glass substrate by using standard electron-beam lithography. The structure with a lattice constant of 600 nm possessed left-handedness and negative refraction at infrared frequencies. In Ref. [16] it was shown that by choosing a proper geometrical shape of the dielectric inclusions, an all-dielectric LHM can be achieved by using single-sized dielectric resonators. Besides, both the left-handedness and the negative refraction phenomenon at far infrared frequencies were observed in a periodic stack of antiferromagnetic and ionic-crystal layers [34] and in graphene-sheet periodic structures [17]. A design for active LHM collaborated with microwave varactors was proposed and experimentally realized in Ref. [35].

It should be noted that a lot of work has been done on the theoretical study of electromagnetic properties of LHMs (see, e.g., Refs. [36–40]). Specifically, in Ref. [36], an analytical theory of low-frequency electromagnetic waves in metallic photonic crystals with a small volume fraction of a metal was presented. The effective medium theory of LHMs based on the transfer matrix calculations on metamaterials of finite lengths was proposed in Ref. [37]. Linear and nonlinear wave propagation in LHMs was theoretically analyzed and a number of nonlinear optical effects were predicted in Ref. [38]. In our opinion, special attention should be paid to Refs. [39–42], in which the effects of Cherenkov radiation and electron-beam instability were theoretically investigated. In Ref. [39], Cherenkov radiation of bulk and surface electromagnetic waves by an electron bunch that moved in vacuum above a composite medium was theoretically investigated. It was shown that Cherenkov radiation gave rise to simultaneous excitation of bulk and surface electromagnetic waves over one and the same frequency range. The excited surface electromagnetic waves can be of two different types: namely, the electric and magnetic ones. The instability of two electron beams passing through a slab of LHM was predicted in Ref. [40]. It was shown that this instability originates from the backward Cherenkov radiation and results in a self-modulation of the beams and radiation of electromagnetic waves. In Ref. [41] the theoretical analysis of excitation of the surface plasmon polaritons by a thin electron beam propagating in the vacuum gap separating a plasmalike medium (metal) from an artificial dielectric with negative magnetic permeability was performed. It was demonstrated that the interface-localized waves with the negative total energy flux could be excited. The case of uniform motion of the charge in infinite LHM was considered in Ref. [42]. Using complex function theory methods, the total field was decomposed into a "quasi-Coulomb" field, a wave field (Cherenkov radiation), and a "plasma trace." It was shown that the wave field in LHM lags behind the charge more so than it does in an ordinary medium.

The LHMs are promising for up-to-date applications, such as amplifiers of evanescent waves [43], magnetic-optical recorders [44], directional antennas [45], and for suppression wake fields that occur during the process of particle acceleration [46,47].

In the present paper, the interaction between a tubular beam of charged particles and eigenmodes of cylindrical dispersive medium are theoretically investigated. This medium may have negative values of ε and μ over a certain frequency range. It will be shown that the interaction gives rise to the absolute instability of the so-called bulk-surface electromagnetic waves, which are the propagating waves in the medium and, at the same time, they are evanescently confined along the normal to the lateral cylinder surface in vacuum. This means that LHMs can be used as the delaying media with "natural feedback" for generation of electromagnetic waves in backward-wave tubes. Besides, the possibility of generation of weakly damped whispering gallery waves will allow the generation of electromagnetic waves in the submillimeter region of the spectrum.

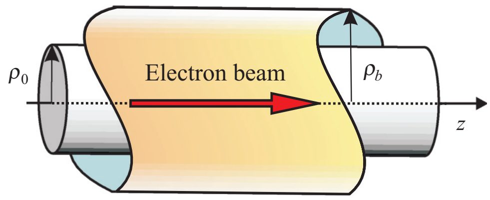

FIG. 1. Geometry of electrodynamic system.

II. STATEMENT OF THE PROBLEM AND BASIC EQUATIONS

Consider an infinite along the z-axis cylinder with the radius ρ_0 occupying the region $0 \leqslant \rho \leqslant \rho_0, 0 \leqslant \varphi \leqslant 2\pi$, and $-\infty \leqslant z \leqslant +\infty$ (see Fig. 1). We suppose that the cylinder is made of a metamaterial with the frequency-dependent permittivity ε and permeability μ, which have negative values over one and the same frequency range. The frequency dependences for $\varepsilon(\omega)$ and $\mu(\omega)$ will be specified below. A tubular electron beam with the radial thickness a and density $N_0(\rho)$ moves in vacuum at a distance of ρ_b from the cylinder axis at a velocity v_0. The quasineutrality condition for the beam is satisfied because the charges of electrons are compensated by the background of positive charges. We assume that the thickness of the beam a is much smaller than the other spatial scales of the electrodynamic system under consideration. Hence the undisturbed beam density can be represented as $N_0(\rho) = N_0 a\delta(\rho - \rho_b)$, where N_0 is the equilibrium beam density and $\delta(\rho - \rho_b)$ is the Dirac delta function.

Below we will consider the interaction between the electron beam and the cylinder eigenmodes in a linear approximation. In this case, we specify the disturbed beam current density at a point with the radius-vector $\mathbf{r}$ at a moment t as

$$\mathbf{j}(\mathbf{r},t) = eN_0(\rho)\mathbf{v}(\mathbf{r},t) + e\mathbf{v}_0 N(\mathbf{r},t),$$

where e is the electron charge, and $N(\mathbf{r},t)$ and $\mathbf{v}(\mathbf{r},t)$ are the variable components of the beam density and the electron velocity, respectively. Hereafter, we will suppose the radial component of the beam current density is equal to zero because of the chosen model of the electron beam.

To describe the interaction between the electron beam and the cylinder eigenmodes, we take as a starting point the following Maxwell equations together with the linearized continuity and motion equations for the beam electrons:

$$\mathrm{rot}\mathbf{H}(\mathbf{r},t) = \frac{1}{c}\frac{\partial}{\partial t}\mathbf{D}(\mathbf{r},t) + \frac{4\pi}{c}\mathbf{j}(\mathbf{r},t), \tag{1}$$

$$\mathrm{rot}\mathbf{E}(\mathbf{r},t) = -\frac{1}{c}\frac{\partial}{\partial t}\mathbf{B}(\mathbf{r},t), \tag{2}$$

$$\mathrm{div}\mathbf{D}(\mathbf{r},t) = 4\pi eN(\mathbf{r},t), \tag{3}$$

$$\mathrm{div}\mathbf{B}(\mathbf{r},t) = 0, \tag{4}$$

$$e\frac{\partial N(\mathbf{r},t)}{\partial t} + \mathrm{div}\mathbf{j}(\mathbf{r},t) = 0, \tag{5}$$

$$\frac{\partial \mathbf{v}(\mathbf{r},t)}{\partial t} + v_0\frac{\partial \mathbf{v}(\mathbf{r},t)}{\partial z} = \frac{e}{m}\left\{\mathbf{E}(\mathbf{r},t) + \frac{1}{c}[\mathbf{v}_0,\mathbf{B}(\mathbf{r},t)]\right\}, \tag{6}$$

where m is the electron mass, c is the velocity of light in vacuum, $\mathbf{E}(\mathbf{r},t)$ and $\mathbf{H}(\mathbf{r},t)$ are the electric and magnetic field vectors, and $\mathbf{D}(\mathbf{r},t)$ and $\mathbf{B}(\mathbf{r},t)$ are the electric displacement and magnetic induction vectors that are related with the $\mathbf{E}(\mathbf{r},t)$- and $\mathbf{H}(\mathbf{r},t)$-vectors by the constitutive equations

$$\mathbf{D}(\mathbf{r},t) = \int_{-\infty}^{t} \tilde{\varepsilon}(t - t')\mathbf{E}(\mathbf{r},t')dt', \tag{7}$$

$$\mathbf{B}(\mathbf{r},t) = \int_{-\infty}^{t} \tilde{\mu}(t - t')\mathbf{H}(\mathbf{r},t')dt', \tag{8}$$

where $\tilde{\varepsilon}(t - t')$ and $\tilde{\mu}(t - t')$ are the influence functions that characterize the efficiency of the field action in time. Note that the difference nature of the kernels of the integrals is due to the homogeneity of the metamaterial properties in time.

In order to derive the dispersion equation for the electromagnetic waves in the electrodynamic system under consideration, it is necessary to satisfy certain boundary conditions at $\rho = \rho_0$ and $\rho = \rho_b$. These conditions are as follows. First, the tangential components of the electric and magnetic fields are continuous at $\rho = \rho_0$. Second, at $\rho = \rho_b$ the tangential components of the magnetic fields are discontinuous because of the beam current. Note that the normal component of the magnetic induction vector remains continuous, whereas the normal component of the electric displacement vector suffers discontinuity because of the disturbed beam charge.

We determine the discontinuities of the tangential components of the magnetic field and the normal component of the electric displacement [in vacuum $D_\rho(\mathbf{r},t) \equiv E_\rho(\mathbf{r},t)$] by integrating Eqs. (1) and (3) over the infinitesimally small beam thickness. As a result, we have

$$H_\varphi(\mathbf{r},t)\big|_{\rho=\rho_b+0} - H_\varphi(\mathbf{r},t)\big|_{\rho=\rho_b-0} = \frac{4\pi}{c\rho_b}\lim_{\Delta\rho\to 0}\int_{\rho_b-\Delta\rho}^{\rho_b+\Delta\rho} j_z(\mathbf{r},t)\rho d\rho, \tag{9}$$

$$H_z(\mathbf{r},t)|_{\rho=\rho_b+0} - H_z(\mathbf{r},t)|_{\rho=\rho_b-0} = -\frac{4\pi}{c}\lim_{\Delta\rho\to 0}\int_{\rho_b-\Delta\rho}^{\rho_b+\Delta\rho} j_\varphi(\mathbf{r},t)d\rho, \tag{10}$$

$$E_\rho(\mathbf{r},t)\big|_{\rho=\rho_b+0} - E_\rho(\mathbf{r},t)\big|_{\rho=\rho_b-0} = \frac{4\pi e}{\rho_b}\lim_{\Delta\rho\to 0}\int_{\rho_b-\Delta\rho}^{\rho_b+\Delta\rho} N(\mathbf{r},t)\rho d\rho. \tag{11}$$

We represent all variables in the form of the set of space-time harmonics, for instance,

$$\mathbf{E}(\mathbf{r},t) = \sum_{n=-\infty}^{\infty}\int_{-\infty}^{\infty}\int_{-\infty}^{\infty}\mathbf{E}_n(\rho,q_z,\omega) \times \exp\left[i(q_z z + n\varphi - \omega t)\right]dq_z d\omega, \tag{12}$$

where ω, q_z, and n are the frequency, longitudinal wave number, and the number of the spatial harmonic (coinciding with the azimuthal mode index), respectively; $i^2 = -1$.

If we take into account Eq. (12), we can rewrite the original equations, Eqs. (1)–(4), for the axial spectral components of the field in the region outside the electron beam ($\rho \neq \rho_b$) in the following form:

$$\left[\frac{1}{\rho}\frac{\partial}{\partial\rho}\rho\frac{\partial}{\partial\rho}+\left(q_\nu^2-\frac{n^2}{\rho^2}\right)\right]\left\{\begin{matrix}E_{\nu,zn}(\rho,q_z,\omega)\\ H_{\nu,zn}(\rho,q_z,\omega)\end{matrix}\right\}=0, \quad (13)$$

where $\nu = 1$ for the cylinder region and $\nu = 2$ for vacuum; $q_\nu^2 = \varepsilon_\nu\mu_\nu\omega^2/c^2 - q_z^2$ is the square of the transverse wave number of electromagnetic waves. When $q_\nu^2 > 0$, the system of equations (13) has the form of the Bessel equations, whereas when $q_\nu^2 < 0$ they are the modified Bessel equations. Hereinafter we take the following notations: $q_1^2 = \kappa^2 = \varepsilon\mu\omega^2/c^2 - q_z^2$ in the cylinder region and $q_2^2 = q^2 = \omega^2/c^2 - q_z^2$ in vacuum.

Hereafter, we will use the frequency dependencies $\varepsilon(\omega)$ and $\mu(\omega)$ the same as in Refs. [8,10]:

$$\varepsilon(\omega) = 1-\frac{\omega_L^2}{\omega^2},\quad \mu(\omega)=1-\frac{F\omega^2}{\omega^2-\omega_r^2}, \quad (14)$$

where ω_L is the effective plasma frequency, ω_r is the resonance frequency, F is the fractional area of the metamaterial unit cell occupied by the interior of the split ring resonator, and $F < 1$. We recall that because these resonators respond to the incident magnetic field, the medium can be viewed as having an effective permeability (see Ref. [10]).

We are only interested in the waves, which are evanescently confined along the normal to the lateral cylinder surface in vacuum. For these waves the condition $q^2 < 0$ is satisfied. Exactly, these waves are excited by the beam of charged particles provided the Cherenkov resonance $\omega = q_z v_0$. Indeed, for the nonrelativistic electron velocities ($\beta \ll 1$, where $\beta = v_0/c$ is the dimensionless electron velocity) considered herein, we have $\omega^2/c^2 \ll q_z^2$ and $q^2 < 0$. Taking into account the aforesaid, we represent the expressions for the spectral components of the electromagnetic field $E_{zn}(\rho,q_z,\omega)$ and $H_{zn}(\rho,q_z,\omega)$ in the following form:

$$E_{zn}(\rho,q_z,\omega) = \begin{cases}\begin{cases}A_n^E J_n(\kappa\rho), & \kappa^2>0\\ A_n^E I_n(|\kappa|\rho), & \kappa^2<0\end{cases}, & \rho\leqslant\rho_0\\ B_n^E K_n(|q|\rho)+C_n^E I_n(|q|\rho), & \rho_0<\rho<\rho_b\\ D_n^E K_n(|q|\rho), & \rho>\rho_b\end{cases}, \quad (15)$$

$$H_{zn}(\rho,q_z,\omega) = \begin{cases}\begin{cases}A_n^H J_n(\kappa\rho), & \kappa^2>0\\ A_n^H I_n(|\kappa|\rho), & \kappa^2<0\end{cases}, & \rho\leqslant\rho_0\\ B_n^H K_n(|q|\rho)+C_n^H I_n(|q|\rho), & \rho_0<\rho<\rho_b\\ D_n^H K_n(|q|\rho), & \rho>\rho_b\end{cases}, \quad (16)$$

where $J_n(u)$ is the nth order Bessel function of the first kind; $I_n(u)$ and $K_n(u)$ are the modified functions of the first kind (Infeld function) and the second kind (Macdonald function), respectively [48]; $A_n^{E,H}$, $B_n^{E,H}$, $C_n^{E,H}$, and $D_n^{E,H}$ are the arbitrary constants. The choice of the solution is due to the fulfillment of finiteness conditions for $E_{zn}(\rho,q_z,\omega)$ and $H_{zn}(\rho,q_z,\omega)$ at $\rho \to 0$ and $\rho \to \infty$. At $\beta^2\varepsilon\mu > 1$ the expressions for the components $E_{zn}(\rho,q_z,\omega)$ and $H_{zn}(\rho,q_z,\omega)$ of the fields inside the cylinder are described by Bessel functions $J_n(\kappa\rho)$, and at $\beta^2\varepsilon\mu < 1$ they are described by modified Bessel functions $I_n(|\kappa|\rho)$. According to the terminology of Ref. [6], in the first case we term the electromagnetic waves as the bulk-surface waves, whereas in the second case the electromagnetic waves are represented as the surface waves. Using the Maxwell equations, we express other Fourier components of the electromagnetic fields in the cylinder region ($\rho < \rho_0$), as well as in the annular gap ($\rho_0 < \rho < \rho_b$), and on the other side of the beam ($\rho > \rho_0$) via the components $E_{zn}(\rho,q_z,\omega)$ and $H_{zn}(\rho,q_z,\omega)$.

We note that in the nonrelativistic case, when $\beta^2 \ll 1$ and $\varepsilon\mu\beta^2 > 1$, the discontinuities of the tangential magnetic field components $H_{\varphi n}(\rho,q_z,\omega)$ and $H_{zn}(\rho,q_z,\omega)$ at the beam surface ($\rho = \rho_b$) are small values of the order of $O(\beta)$. Therefore, in what follows, in the boundary conditions at the beam surface ($\rho = \rho_b$), we suppose these components are continuous, and take into account only the discontinuity of the electric field component $E_{\rho n}(\rho,q_z,\omega)$.

Assuming the beam is nonrelativistic, and satisfying the above-mentioned boundary conditions at the cylinder and electron beam surfaces, we obtain the following dispersion equation for the beam-cylinder coupled waves:

$$\Delta\left[(\omega-q_z v_0)^2-\Gamma(q_z,n)\omega_b^2\right]=\alpha\omega_b^2, \quad (17)$$

where $\omega_b = \sqrt{4\pi e^2 N_0/m}$ is the plasma frequency of beam electrons, $\Gamma(q_z,n)$ is the depression factor of space-charge forces [2], and

$$\Gamma(q_z,n)=\frac{a}{\rho_b}\left(n^2+q_z^2\rho_b^2\right)I_n(|q_z|\rho_b)K_n(|q_z|\rho_b)\times\left[1-\frac{I_n(|q_z|\rho_0)K_n(|q_z|\rho_b)}{I_n(|q_z|\rho_b)K_n(|q_z|\rho_0)}\right]. \quad (18)$$

α is the coupling factor of the beam with cylinder eigenmodes that has the form

$$\alpha=\frac{a}{\rho_b}\left(n^2+q_z^2\rho_b^2\right)\frac{K_n^2(|q_z|\rho_b)}{q_z^2\rho_0^2K_n^2(|q_z|\rho_0)}\Delta^H, \quad (19)$$

$$\Delta=\Delta_0-\Delta^E\Delta^H, \quad (20)$$

$$\Delta_0=\left[\frac{nq_z\omega(\varepsilon\mu-1)}{q^2\kappa^2\rho_0^2c}\right]^2, \quad (21)$$

$$\Delta^E=\frac{1}{|q|\rho_0}\frac{K_n'(|q|\rho_0)}{K_n(|q|\rho_0)}+\frac{\varepsilon}{\kappa\rho_0}\frac{J_n'(\kappa\rho_0)}{J_n(\kappa\rho_0)},$$
$$\Delta^H=\frac{1}{|q|\rho_0}\frac{K_n'(|q|\rho_0)}{K_n(|q|\rho_0)}+\frac{\mu}{\kappa\rho_0}\frac{J_n'(\kappa\rho_0)}{J_n(\kappa\rho_0)}. \quad (22)$$

Note that Eq. (17) has the form analogous to the characteristic equation of a traveling-wave tube [2]. In our case, it describes the interaction of the beam space-charge waves (SCWs) with the cylinder eigenmodes. Dispersion equations for the beam SCWs and the cylinder eigenmodes are described by the following equations:

$$(\omega-q_z v_0)^2-\Gamma(q_z,n)\omega_b^2=0,\ \text{and}\ \ \Delta=0. \quad (23)$$

The equation $\Delta = 0$ can be interpreted as the dispersion equation of hybrid E- and H-type waves. The symmetric ($n =$

0) cylinder E-type eigenmodes are characterized by the equation $\Delta^E = 0$, whereas the symmetric H-type waves are characterized by the equation $\Delta^H = 0$. For hybrid E- and H-type waves the conditions $|E_{zn}(\rho,q_z,\omega_p)|_{\max}/|H_{zn}(\rho,q_z,\omega_p)|_{\max} > 1$ and $|E_{zn}(\rho,q_z,\omega_p)|_{\max}/|H_{zn}(\rho,q_z,\omega_p)|_{\max} < 1$ (where the index "max" indicates the maximum value of the corresponding component) are satisfied, respectively. From these facts, it transpires that the wave type is determined by the dominant axial component of the electromagnetic field [49]. In the mode double subscript $p \equiv ns$; the radial index s represents the number of field variations along the radial coordinate and corresponds to the pair of roots order number of the equation $\Delta = 0$, whose solutions determine the frequencies ω_p of the cylinder eigenmodes with the longitudinal wave number q_z. In the case of symmetric waves, the index s corresponds to the root order number of the corresponding dispersion equation: $\Delta^E = 0$ or $\Delta^H = 0$. In the dispersion equation $\Delta = 0$ the role of the coupling factor between the E and H waves is played by the quantity Δ_0. If $n = 0$, the dispersion equation $\Delta = 0$ splits into two independent equations $\Delta^E = 0$ and $\Delta^H = 0$. In this case, the electromagnetic fields of symmetric waves have three components: $E_{\rho 0s}$, $H_{\varphi 0s}$, and E_{z0s} for E waves, and $H_{\rho 0s}$, $E_{\varphi 0s}$, H_{z0s} for H waves [here $E_{zns} \equiv E_{zn}(\rho,q_z,\omega_p)$, $H_{zns} \equiv H_{zn}(\rho,q_z,\omega_p)$, etc., where $p \equiv 0s$]. If $n \neq 0$, all electric and magnetic field components of the cylinder eigenmodes are nonzero, and, therefore, they are the hybrid E- and H-type waves.

In the case of $\rho_0 \to 0$ (i.e., the cylinder is absent in the electrodynamic system), we have $\alpha/\Delta \to 0$, and the solutions of the dispersion equation, Eq. (17), determine the frequencies of the slow (ω_-) and fast (ω_+) beam SCWs:

$$\omega_- = q_z v_0 - R_0(q_z,n)\omega_b, \tag{24}$$

$$\omega_+ = q_z v_0 + R_0(q_z,n)\omega_b, \tag{25}$$

where $R_0(q_z,n) = \sqrt{\Gamma_0(q_z,n)}$ is the reduction factor [2], and

$$\Gamma_0(q_z,n) = \operatorname*{Lim}_{\rho_0\to 0}\Gamma(q_z,n) = \frac{a}{\rho_b}\left(n^2 + q_z^2\rho_b^2\right) I_n(|q_z|\rho_b)K_n(|q_z|\rho_b). \tag{26}$$

As follows from Eqs. (24) and (25), the phase velocities of the slow and fast SCWs are, respectively, less and greater than the beam velocity v_0.

Our goal is to determine the frequencies of the cylinder eigenmodes and the increments (decrements) of the beam-cylinder coupled waves. When the beam is absent in the system ($\omega_b = 0$), the dispersion equation, Eq. (17), is reduced to the dispersion equation for the cylinder eigenmodes $\Delta = 0$. Hence we determine the cylinder eigenmodes ω_p. The frequencies ω_p are changed because of the interaction of the beam with the cylinder, and, as a result, small frequency corrections $|\delta\omega| \ll \omega_p$ occur. They are small because the plasma frequency of the beam electrons is less than the frequencies of the cylinder eigenmodes ($\omega_b < \omega_p$). Just this case is of interest because the cylinder eigenmodes are excited. Then Eq. (17) can be represented as follows:

$$\delta\omega^3 + 2(\omega_p - q_z v_0)\delta\omega^2 + \left[(\omega_p - q_z v_0)^2 - \Gamma(q_z,n)\omega_b^2\right]\delta\omega - \frac{\alpha(\omega_p)}{\Delta'_\omega(\omega_p)}\omega_b^2 = 0, \tag{27}$$

where $\Delta'_\omega(\omega_p)$ is the frequency derivative of Δ, which is calculated at the cylinder eigenfrequency ω_p. The case of resonances is of the greatest interest. If the electron velocity v_0 satisfies the condition $\omega_p = q_z v_0$ (the Cherenkov resonance [50]) and $\Gamma(q_z,n) = 0$, then from Eq. (27) we obtain

$$\delta\omega^3 = \frac{\alpha(\omega_p)}{\Delta'_\omega(\omega_p)}\omega_b^2. \tag{28}$$

This case is realized if $\rho_b = \rho_0$. If $\rho_b \neq \rho_0$, then Eq. (28) remains valid when the condition $R(q_z,n)\omega_b \ll |\delta\omega|$ [where $R(q_z,n) = \sqrt{\Gamma(q_z,n)}$] is satisfied. The value $R(q_z,n)\omega_b$ makes sense of the effective (or reduced) plasma frequency of the beam [2]. Note that Eq. (28) has three roots, one of which is real and the other two are complex-conjugate roots. One of the complex-conjugate roots has a positive imaginary part, which leads to a wave amplitude rise with time. A root with a negative imaginary part refers to a damped wave with time. From Eq. (28) we determine the following expression for the instability increment:

$$\mathrm{Im}\delta\omega = \frac{\sqrt{3}}{2}\left|\frac{\alpha(\omega_p)}{\Delta'_\omega(\omega_p)}\right|^{1/3}\omega_b^{2/3}. \tag{29}$$

Since, according to Eq. (29), the instability increment is proportional to $N_0^{1/3}$, the excitation of the cylinder eigenmodes by resonant beam particles (whose velocity satisfies the condition $\omega_p = q_z v_0$) is coherent [51]. As noted above, this instability is caused by the Cherenkov effect.

Note that if $\rho_b > \rho_0$ the resonant interaction of the electron beam with the cylinder eigenmodes is possible at frequencies

$$\omega_p^{\pm} = \omega_{\pm} = q_z v_0 \pm R(q_z,n)\omega_b.$$

If the condition $R(q_z,n)\omega_b \gg |\delta\omega|$ is valid, Eq. (27) takes the form

$$\delta\omega^2 = \pm\frac{\alpha(\omega_p^{\pm})\omega_b}{2R(q_z,n)\Delta'_\omega(\omega_p^{\pm})}. \tag{30}$$

In Eq. (30) the plus sign before the fraction corresponds to the frequency ω_p^+, and the minus sign is for the frequency ω_p^-. It is evident that the condition $\delta\omega^2 < 0$ is only valid at the frequencies ω_p^-. This means that the instability emerges only if the slow space-charge wave interacts with the cylinder eigenmodes (the anomalous Doppler effect [50]). The interaction of the fast space-charge wave with the cylinder eigenmodes results only in the appearance of real corrections to the frequencies ω_p^+. Thus Eq. (30) has two real roots for ω_p^+ and two complex-conjugate roots for ω_p^-. The root with a positive imaginary part corresponds to an increasing with time wave. In case of the anomalous Doppler effect, from Eq. (30) we obtain the following expression for the instability increment:

$$\mathrm{Im}\delta\omega = \left[\frac{\alpha(\omega_p^-)\omega_b}{2R(q_z,n)\Delta'_\omega(\omega_p^-)}\right]^{1/2}. \quad (31)$$

It follows from Eq. (31), that the instability increment is proportional to $N_0^{1/4}$.

To gain a better insight into the interaction mechanism of the charged particles of a tubular beam with the cylinder waves, below we present the numerical analysis results of the dispersion equation, Eq. (17), and the expression for the instability increment, Eq. (29), corresponding to Cherenkov resonance. The fact is that waves excited under the Cherenkov resonance conditions are characterized by greater instability increments (by ten or more times) than the waves excited under the anomalous Doppler effect conditions.

III. NUMERICAL ANALYSIS OF THE DISPERSION EQUATION

It is convenient to carry out a numerical analysis of the dispersion equation, Eq. (17), using the following dimensionless quantities: $\bar{\kappa} = \kappa\rho_0$, $\bar{q} = q\rho_0$, $\bar{q}_z = q_z\rho_0$, $\bar{\rho}_b = \rho_b/\rho_0$, $\bar{a} = a/\rho_0$, $\bar{\omega} = \omega/\omega_0$, $\bar{\omega}_L = \omega_L/\omega_0$, and $\bar{\omega}_r = \omega_r/\omega_0$, where $\omega_0 = c/\rho_0$. In calculations, we choose the following geometric and material parameters of the cylinder: $\rho_0 = 0.5\,\mathrm{cm}$, $F = 0.56$, $\bar{\omega}_L = 2$, $\bar{\omega}_r = 1$, and $\bar{\omega}_{\mu=0} = \omega_{\mu=0}/\omega_0 \approx 1.51$ (it is the frequency at which $\mu = 0$). The values of the equilibrium beam electron density N_0, the radial thickness of the beam a, and the directed motion velocity of the beam electrons are chosen as follows: $N_0 = 7.6 \times 10^{10}\,\mathrm{cm}^{-3}$, $a = 0.05\,\mathrm{cm}$, and $v_0 = 0.3c$, respectively. For the selected system parameters, we have $\omega_0 = 6 \times 10^{10}\,\mathrm{s}^{-1}$, and $\omega_b^2/\omega_0^2 \approx 0.07$, and the value $\bar{q}_z = 1$ refers to $q_z = 2\,\mathrm{cm}^{-1}$ and the corresponding wavelength $\lambda = 2\pi/q_z = \pi$ cm.

A. Spectra of the cylinder eigenmodes

Before proceeding to the analysis of the dispersion characteristics of the cylinder eigenmodes, let us analyze the frequency dependences of ε and μ shown in Fig. 2. Curves 1 and 2 correspond to the dependences $\varepsilon(\bar{\omega})$ and $\mu(\bar{\omega})$, respectively. Curve 3 corresponds to the value $\mu(\bar{\omega}) = 1 - F$. Straight lines 4, 5, and 6 correspond to the frequencies $\bar{\omega} = \bar{\omega}_r$, $\bar{\omega} = \bar{\omega}_{\mu=0}$, and $\bar{\omega} = \bar{\omega}_L$, respectively. In Fig. 2 there are the following four frequency regions depending on the combinations of the signs of $\varepsilon(\bar{\omega})$ and $\mu(\bar{\omega})$: (I) $0 < \bar{\omega} < \bar{\omega}_r$, where $\varepsilon < 0$, $\mu > 0$; (II) $\bar{\omega}_r < \bar{\omega} < \bar{\omega}_{\mu=0}$, where $\varepsilon < 0$, $\mu < 0$; (III) $\bar{\omega}_{\mu=0} < \bar{\omega} < \bar{\omega}_L$, where $\varepsilon < 0$, $\mu > 0$; (IV) $\bar{\omega} > \bar{\omega}_L$, where $\varepsilon > 0$, $\mu > 0$. The permeability $\mu(\bar{\omega})$ tends to plus or minus infinity at $\bar{\omega} \to \bar{\omega}_r - 0$ or $\bar{\omega} \to \bar{\omega}_r + 0$, respectively.

Since in the frequency region I the conditions $\kappa^2 < 0$ and $\Delta^H < 0$ are simultaneously satisfied then only E-type surface electromagnetic waves can exist in it.

In frequency region II, the conditions $\varepsilon < 0$ and $\mu < 0$ are simultaneously satisfied. Therefore the cylinder metamaterial behaves like the left-handed medium. In this frequency range, the conditions $\kappa^2 < 0$ and $\kappa^2 > 0$ can simultaneously be satisfied. This fact means the possibility of the simultaneous existence of bulk-surface and surface electromagnetic waves at the same frequency, but with different values of the wave number q_z. The analogous feature of the left-handed medium properties, namely, the ability to sustain the existence (at the same frequency) of bulk-surface and surface waves in case of a plane interface between a left-handed medium and a vacuum, was demonstrated in Refs. [39,52].

In frequency region III, just as in the frequency region I, the conditions $\kappa^2 < 0$ and $\Delta^H < 0$ are simultaneously valid. Therefore, only the E-type surface electromagnetic waves can exist.

In frequency region IV, the condition $\kappa^2 > 0$ holds and, consequently, the E- and H-type bulk-surface waves can only exist. When the condition $\kappa^2 < 0$ holds we have $\Delta^E < 0$ and $\Delta^H < 0$ which indicates the absence of solutions of dispersion equations $\Delta^E = 0$ and $\Delta^H = 0$. It follows that it is not possible that the surface symmetric ($n = 0$) electromagnetic waves exist in this frequency range.

Region II is of the greatest interest for us because the cylinder material behaves there like a left-handed medium. Therefore, we will concentrate our attention on studying the features of the dispersion dependences of electromagnetic waves in this frequency region. Hereafter, we will evaluate the roots of corresponding dispersion equations using the simplex method for minimization of a function of several variables [53].

Figure 3 shows the dispersion dependences of the cylinder symmetric eigenmodes ($n = 0$). Straight lines 1, 2, and 3 correspond to $\bar{\omega} = \bar{\omega}_r$ and $\bar{\omega} = \bar{\omega}_{\mu=0}$, and the light line in vacuum $\bar{\omega} = \bar{q}_z$, respectively. Curve 4 corresponds to the solution of the equation $\bar{\kappa} = 0$. Straight lines 5 and 6 represent the frequencies at which $\varepsilon = -1$ and $\mu = -1$, respectively. Curves 7 and 8 refer to the E-type bulk-surface waves, and curves 9 and 10 are for the H-type bulk-surface waves. Curves 11 and 12 are the surface waves of E and H type, respectively. The empty circles show the starting (ending)

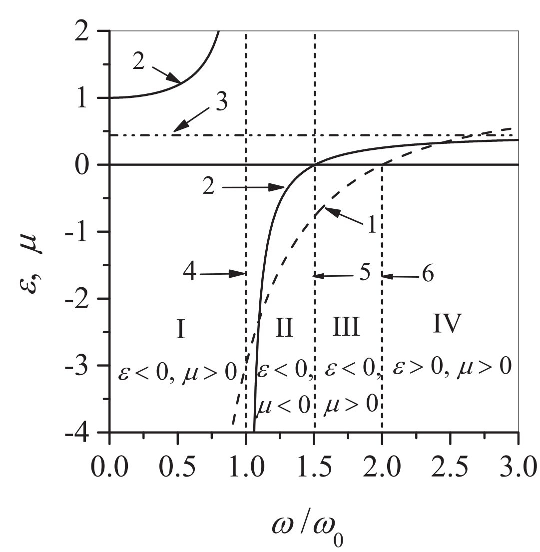

FIG. 2. Frequency dependences $\varepsilon(\bar{\omega})$ and $\mu(\bar{\omega})$. Curves 1 and 2 correspond to the dependences $\varepsilon(\bar{\omega})$ and $\mu(\bar{\omega})$, respectively. Curve 3 corresponds to the value $\mu(\bar{\omega}) = 1 - F$, where $F = 0.56$. Straight lines 4, 5, and 6 correspond to $\bar{\omega}_r = 1$, $\bar{\omega}_{\mu=0} \approx 1.51$, and $\bar{\omega}_L = 2$, respectively.

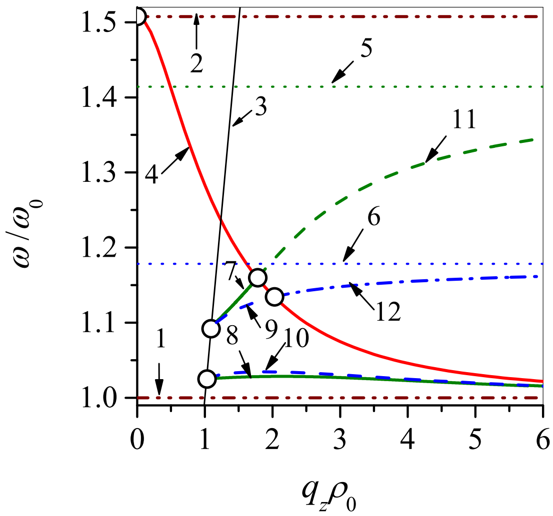

FIG. 3. Dispersion dependences of the cylinder symmetric eigenmodes ($n = 0$) in the frequency region where $\varepsilon < 0$ and $\mu < 0$. Lines 1, 2, and 3 represent straight lines $\bar{\omega}_r = 1$ and $\bar{\omega}_{\mu=0} \approx 1.51$, and the light line in vacuum $\bar{\omega} = \bar{q}_z$, respectively. Curve 4 is for the solution of the equation $\bar{\kappa} = 0$. Straight lines 5 and 6 are for the frequencies at which $\varepsilon = -1$ and $\mu = -1$, respectively. Curves 7 and 8 refer to the E-type bulk-surface waves, and curves 9 and 10 are for the H-type bulk-surface waves. Curves 11 and 12 are for the surface waves of E and H type, respectively. The empty circles show the starting (ending) points of the spectra of corresponding waves.

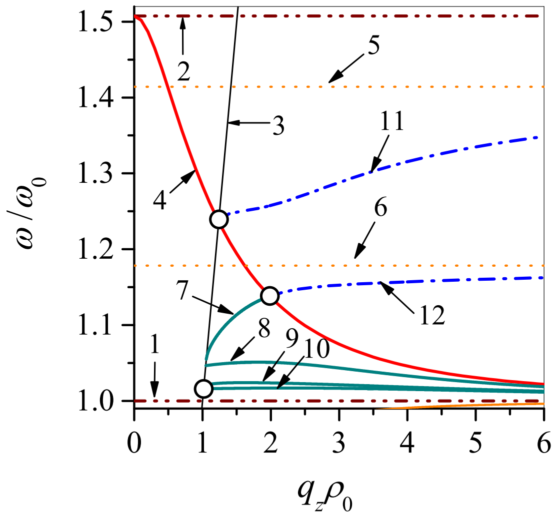

FIG. 4. Dispersion dependences of the cylinder unsymmetrical eigenmodes with the azimuthal index $n = 1$ in the frequency range where $\varepsilon < 0$ and $\mu < 0$. Lines 1–6 are the same as in Fig. 3. Curves 7 and 8 correspond to the hybrid-type bulk-surface modes with the radial index $s = 1$, and curves 9 and 10 are for the bulk-surface hybrid modes with $s = 2$. The empty circles show the starting (ending) points of the spectra of corresponding waves.

points of the spectra of corresponding waves. Generally speaking, the values of $\bar{\omega}$ and $\bar{q}_z$ at these points do not satisfy the corresponding dispersion equations ($\Delta^E = 0$ or $\Delta^H = 0$).

As shown in Fig. 3, the dispersion curves of bulk-surface waves (curves 7–10) are located in the region bounded by the straight lines 1 ($\bar{\omega} = \bar{\omega}_r$) and 3 ($\bar{\omega} = \bar{q}_z$), and curve 4 ($\bar{\kappa} = 0$) where the conditions $\bar{q}^2 < 0$ and $\bar{\kappa}^2 > 0$ are satisfied. These dispersion curves originate from the light line $\bar{\omega} = \bar{q}_z$ in a vacuum. To the left of this line they convert in the dispersion curves of cylinder bulk eigenmodes, when $\bar{q}^2 > 0$, and consequently, the fields in vacuum are described by the Hankel functions of the first kind [49]. These modes cannot be excited by a beam of charged particles moving in a vacuum, since in this case $\bar{q}^2 < 0$. Therefore, they are not of interest to us. The coordinates of the starting points of the spectra of bulk-surface modes on the light line in vacuum for arbitrary values of the index n are determined from the conditions $\bar{\omega} = \bar{q}_z$ and $\Delta = 0$. Since the equation $\Delta = 0$ has infinitely many solutions, there exist infinitely many starting points of the pair of branches of E and H waves. Here, the density of such branches will increase as the frequency $\bar{\omega}$ approaches the resonance value of $\bar{\omega}_r$, when $\kappa \to \infty$. As noted above the order number of the pair of branches of E and H waves corresponds to the mode radial index s. Consequently, in Fig. 3 the value $s = 1$ is for the pair of curves 7 and 9, and the value $s = 2$ is for the pair of curves 8 and 10. Using the classification proposed in Ref. [49], the branches 7 and 9 refer to the E_{01} and H_{01} modes, respectively. Here, the first index corresponds to the value of n, and the second one is for the value s. Similarly, the branches 8 and 10 represent the dispersion dependencies of E_{02} and H_{02} modes, respectively. Note that the dispersion curves with values $s > 2$ that are located in pairs below the curves for E_{02} and H_{02} modes are not shown in Fig. 3.

From Fig. 3, it follows that the dispersion dependences of the bulk-surface modes E_{01} and H_{01} (curves 7 and 9) have normal dispersion, and on the curve $\bar{\kappa} = 0$ they convert to the dispersion curves of the E- (curve 11) and H-type (curve 12) surface waves, respectively. The dispersion dependences of the bulk-surface modes E_{02} and H_{02} (curves 8 and 10) have parts with normal and anomalous dispersion, and if $\bar{q}_z \to \infty$ they approach the straight line $\bar{\omega} = \bar{\omega}_r$ asymptotically. Note that the dispersion dependences of the bulk-surface modes with $s > 2$ are similar to the dependences for the E_{02} and H_{02} modes. Dispersion dependences of the surface E and H waves (curves 11 and 12) have normal dispersion. If $\bar{q}_z \to \infty$, the frequency of the surface E wave (curve 11) approaches asymptotically the frequency at which $\varepsilon = -1$ (line 5), and the frequency of the H wave (curve 12) approaches the frequency at which $\mu = -1$ (line 6).

Let us consider the dispersion dependences of the cylinder unsymmetrical eigenmodes ($n \neq 0$) in the frequency range where $\varepsilon < 0$ and $\mu < 0$. In Fig. 4, the spectra of cylinder eigenmodes with the azimuthal index $n = 1$ are shown. Note that the qualitative behavior of the dispersion dependences of cylinder eigenmodes with $n > 1$ is similar to the dependences for the modes with $n = 1$. The lines 1–6 are the same as in Fig. 3. Curves 7 and 8 correspond to the hybrid-type bulk-surface modes with the radial index $s = 1$, and curves 9 and 10 are for the bulk-surface hybrid modes with $s = 2$. The empty circles show the starting (ending) points of the spectra of corresponding waves. Note that the values of $\bar{\omega}$ and $\bar{q}_z$ at these points do not satisfy the dispersion equation $\Delta = 0$.

As shown in Fig. 4, the dispersion dependences of the bulk-surface waves, labeled by the numbers 8–10, have the parts with both normal and anomalous dispersion. The dispersion dependences of the bulk-surface modes with radial indices $s > 2$ are similar. They are located below the dependences of the hybrid modes with $s = 2$, and in Fig. 4 they are not shown. From Fig. 4, it follows that only one of the dispersion branches of the bulk-surface waves (curve 7) with normal dispersion converts to the branch of the surface wave (curve 12) on the curve $\bar{\kappa} = 0$. If $\bar{q}_z \to \infty$, the frequency of this surface wave approaches asymptotically the frequency at which $\mu = -1$ (line 6). In contrast to the dispersion diagram of the cylinder symmetric waves (Fig. 3), in Fig. 4 the second branch of the surface wave (curve 11), whose frequency tends to the frequency at which $\varepsilon = -1$ (line 5) if $\bar{q}_z \to \infty$, has the starting point at the intersection of the light line $\bar{\omega} = \bar{q}_z$ in vacuum (line 3) and the curve $\bar{\kappa} = 0$ (curve 4).

B. Spectra of coupled waves: Absolute and convective instabilities

Let us ascertain the nature of instability that occurs in the Cherenkov resonant interaction between the electron beam and cylinder eigenmodes under the condition $R(q_z,n)\omega_b \ll |\delta\omega|$ and the condition of an extremely small distance of the beam from the cylinder. Henceforward, we will suppose that $\rho_b = \rho_0$.

It is well known that if for real q_z we find complex ω with $\mathrm{Im}\omega > 0$, a field of monochromatic wave, $\sim \exp[i(q_z z - \omega t)]$, will grow in time without bounds and the electrodynamic system will be unstable [51]. It is apparent that the increase of field amplitude without bounds is valid only in the linear approximation of the electrodynamic system under consideration. At the same time in realistic electrodynamic systems a nonlinear stage in the beam instability develops as the field amplitude increases [54]. There are absolute and convective instabilities. Let us recall that an absolute instability implies the growth of the initial perturbation without bounds for given z as $t \to \infty$. If, however, the perturbation remains bounded for given z and $t \to \infty$, one talks about a convective instability. These instabilities find wide use in generation and amplification of electromagnetic waves (see, e.g., [1–3,51]).

Now our goal is to establish the nature of the instability in a small vicinity of the intersection points of the eigenmode dispersion curves with the beam wave $\bar{\omega} = \bar{q}_z\beta$ (the so-called resonance points). Hereafter, we use the well-known Sturrock method [51,55]. To this end, we represent the values of $\bar{\omega}$ and $\bar{q}_z$ near the resonance points $(\bar{q}_{z,\mathrm{res}},\bar{\omega}_{\mathrm{res}})$ in the following way:

$$\bar{\omega} = \bar{\omega}_{\mathrm{res}} + \delta\bar{\omega}, \quad \bar{q}_z = \bar{q}_{z,\mathrm{res}} + \delta\bar{q}_z, \qquad (32)$$

where $|\delta\bar{\omega}| \ll \bar{\omega}_{\mathrm{res}}$ and $|\delta\bar{q}_z| \ll \bar{q}_{z,\mathrm{res}}$.

For the sake of simplicity and without loss of physical generality, we only consider the case of symmetric modes (where $n = 0$). Substituting expressions from Eq. (32) into Eq. (17) and performing the necessary expansions in terms of small variations of $\delta\bar{q}_z$ and $\delta\bar{\omega}$ about the corresponding resonance values, we obtain the following equation:

$$(\delta\bar{\omega} - \beta\delta\bar{q}_z)^2(\delta\bar{\omega} - \bar{v}_{gr}\delta\bar{q}_z) = \bar{a}\bar{\omega}_b^2\left(\frac{\partial\Delta^E}{\partial\bar{\omega}}\right)^{-1}_{\bar{q}_{z,\mathrm{res}},\bar{\omega}_{\mathrm{res}}}, \qquad (33)$$

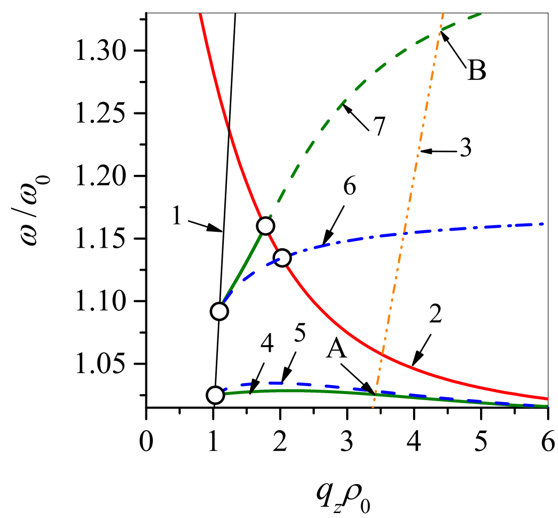

FIG. 5. Dispersion curves of the symmetric eigenmodes and the beam wave. Line 1 refers to the light line in vacuum, curve 2 is for $\bar{\kappa} = 0$, and line 3 is for the beam wave ($\bar{\omega} = \bar{q}_z\beta$). Curves 4 and 5 correspond to the bulk-surface waves H_{02} and E_{02}, respectively, and curves 6 and 7 are for the surface waves of H and E type, respectively. Points A and B correspond to the intersection of the dispersion dependence of the beam wave with the dispersion curves of the bulk-surface wave E_{02} and with the E-type surface wave, respectively.

where $\bar{v}_{gr} = -(\frac{\partial\Delta^E}{\partial\bar{q}_z})_{\bar{q}_{z,\mathrm{res}},\bar{\omega}_{\mathrm{res}}}(\frac{\partial\Delta^E}{\partial\bar{\omega}})^{-1}_{\bar{q}_{z,\mathrm{res}},\bar{\omega}_{\mathrm{res}}}$ is the dimensionless group velocity (in units of the velocity of light in vacuum) of the electromagnetic wave; the values of $(\partial\Delta^E/\delta\bar{q}_z)_{\bar{q}_{z,\mathrm{res}},\bar{\omega}_{\mathrm{res}}}$ and $(\partial\Delta^E/\delta\bar{\omega})_{\bar{q}_{z,\mathrm{res}},\bar{\omega}_{\mathrm{res}}}$ are the corresponding partial derivatives of Δ^E calculated at the resonance point $(\bar{q}_{z,\mathrm{res}},\bar{\omega}_{\mathrm{res}})$. It is worthwhile to emphasize that only symmetric E-type eigenmodes (when $n = 0$) are unstable because their electromagnetic fields have nonzero components of the electric field E_z. Note that only these components cause the interaction between the metamaterial eigenmodes and the nonrelativistic beam electrons. All further results remain valid for the excitation of unsymmetrical eigenmodes ($n \neq 0$) near the corresponding resonance points.

Let us consider the instability regions of the electrodynamic system under consideration near the points of intersection of the dispersion dependence for the beam wave ($\bar{\omega} = \bar{q}_z\beta$) with the dispersion curves of symmetric E-type bulk-surface waves and with the dispersion curve of the E-type surface wave.

Figure 5 presents the dispersion dependencies of the symmetric eigenmodes and the beam wave. Line 1 refers to the light line in vacuum ($\bar{\omega} = \bar{q}_z$), curve 2 is for $\bar{\kappa} = 0$, and line 3 is for the beam wave ($\bar{\omega} = \bar{q}_z\beta$). Curves 4 and 5 correspond to the bulk-surface waves H_{02} and E_{02}, respectively, and curves 6 and 7 are for the surface waves of H and E type, respectively. Points A and B correspond to the intersection of the dispersion dependence of the beam wave with the dispersion curve of the bulk-surface wave E_{02} and with the E-type surface wave, respectively.

Figure 6 presents the dispersion dependencies of the wave [which are the solutions of Eq. (33)] excited by the beam in a small area in the vicinity of point A with coordinates

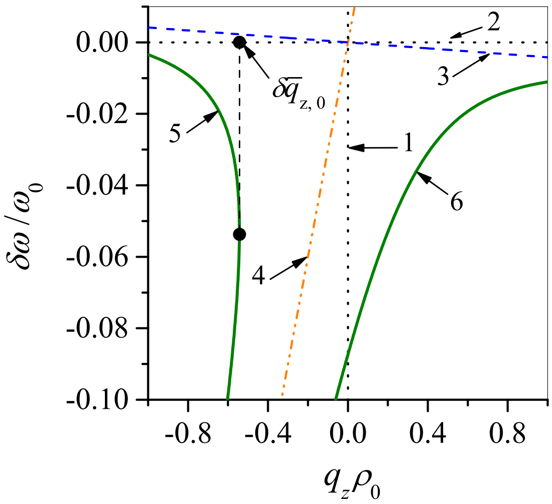

FIG. 6. Dispersion curves of the wave E_{02} excited by the beam in a small area in the vicinity of point A with coordinates $\bar{q}_{z,\mathrm{res}} = 1.025$ and $\bar{\omega}_{\mathrm{res}} = 3.42$. Lines 1 and 2 refer to the values $\delta\bar{q}_z = 0$ and $\delta\bar{\omega} = 0$, line 3 is for the asymptote $\delta\bar{\omega} = \bar{v}_{gr}\delta\bar{q}_z$, line 4 is for $\delta\bar{\omega} = \beta\delta\bar{q}_z$, and curves 5 and 6 are for the wave E_{02} excited by the beam. It is seen that the absolute instability occurs.

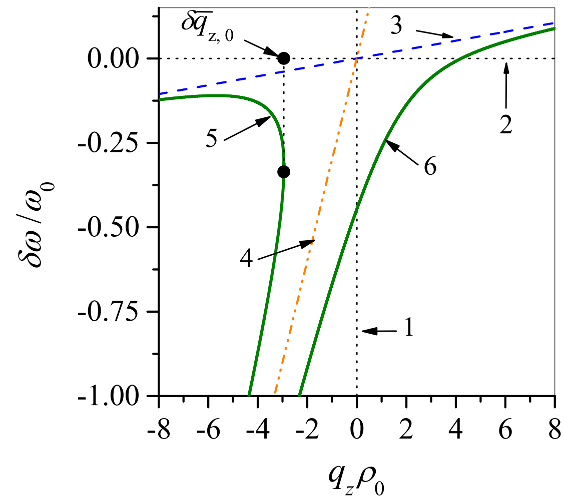

FIG. 7. Dispersion curves of the E-type surface wave excited by the beam in a small area in the vicinity of point B with coordinates $\bar{q}_{z,\mathrm{res}} \approx 4.39$ and $\bar{\omega}_{\mathrm{res}} \approx 1.32$. Lines 1 and 4 have the same meaning as those in Fig. 6. Curves 5 and 6 correspond to the dispersion curves of the E-type surface wave excited by the beam. It is seen that the convective instability occurs.

$\bar{q}_{z,\mathrm{res}} = 1.025$ and $\bar{\omega}_{\mathrm{res}} = 3.42$. Lines 1 and 2 refer to the values $\delta\bar{q}_z = 0$ and $\delta\bar{\omega} = 0$, line 3 is for the asymptote $\delta\bar{\omega} = \bar{v}_{gr}\delta\bar{q}_z$, line 4 is for $\delta\bar{\omega} = \beta\delta\bar{q}_z$, and curves 5 and 6 are for the wave E_{02} excited by the beam.

Since the dispersion equation, Eq. (33), is a cubic one, then, as known, it has three different real roots or one real root and two complex-conjugate roots [56]. As one of these complex roots has a positive imaginary part, the instability develops. As seen from Fig. 6, the instability occurs at all values of δq_z that are greater than $\delta q_{z,0}$. It is also seen that asymptotes 3 and 4 are inclined in different directions with respect to line 2. The negative slope of asymptote 3 is caused by the negative value of the group velocity of corresponding mode ($\bar{v}_{gr} \approx -4.2 \times 10^{-3}$). In accordance with the first Sturrock rule (see Ref. [51,55]) this signifies the occurrence of the absolute instability.

Figure 7 shows the dispersion dependencies of the E-type surface wave excited by the beam in a small area in the vicinity of point B with coordinates $\bar{q}_{z,\mathrm{res}} \approx 4.39$ and $\bar{\omega}_{\mathrm{res}} \approx 1.32$. Lines 1–4 have the same meaning as those in Fig. 6. Curves 5 and 6 correspond to the dispersion curves of the E-type surface wave excited by the beam.

From Fig. 7 it follows that the instability occurs at all values of δq_z greater than $\delta q_{z,0}$. Unlike the case shown in Fig. 6, asymptotes 3 and 4 are inclined in the same direction with respect to line 2. The positive slope of asymptote 3 is caused by the positive value of the group velocity of corresponding mode. In accordance with the first Sturrock rule (see Refs. [51,55]) this means the occurrence of the convective instability.

C. Analysis of instability increments

Let us dwell on the dependences of instability increments $\delta\bar{\omega}$ for bulk-surface waves on the values of azimuthal n and radial s mode indices. These increment values are calculated using the formula Eq. (29). Before moving on, we want to briefly remark on the type of waves excited by a beam. As noted above, if $n = 0$ the beam excites the symmetric E_{0s} modes with radial indices $s \geqslant 2$. If $n \geqslant 1$ the cylinder eigenmodes have nonzero values of all electromagnetic field components and, therefore, they are the hybrid-type modes. In Refs. [49,57], a method was provided for the separation of such modes into the so-called HE_{ns} and EH_{ns} modes depending on the predominant axial component of the electromagnetic field, i.e., the ratio of the maximum values of field components $|E_{zn}(\rho,q_z,\omega_p)|_{\max}$ and $|H_{zn}(\rho,q_z,\omega_p)|_{\max}$. If the axial component of the electric field dominates ($|E_{zn}(\rho,q_z,\omega_p)|_{\max}/|H_{zn}(\rho,q_z,\omega_p)|_{\max} > 1$), the eigenmode is the HE_{ns} mode (E type); otherwise it is the EH_{ns} mode (H type). Numerical analysis of excited modes with azimuthal indices $n \geqslant 1$ shows that in the resonance points, in which $\bar{q}_z = \bar{q}_{z,\mathrm{res}}$ and $\bar{\omega}_p = \bar{\omega}_{\mathrm{res}}$, we have $|E_{zn}(\bar{\rho},\bar{q}_{z,\mathrm{res}},\bar{\omega}_{\mathrm{res}})|_{\max}/|H_{zn}(\bar{\rho},\bar{q}_{z,\mathrm{res}},\bar{\omega}_{\mathrm{res}})|_{\max} > 1$. This implies that in a cylinder made of a metamaterial with $\varepsilon(\bar{\omega}) < 0$ and $\mu(\bar{\omega}) < 0$ the nonrelativistic ($\beta \ll 1$) electron beam excites the E-type eigenmodes.

As a matter of fact, the analytic estimations of the ratio $|E_{zn}(\bar{\rho},\bar{q}_{z,\mathrm{res}},\bar{\omega}_{\mathrm{res}})|_{\max}/|H_{zn}(\bar{\rho},\bar{q}_{z,\mathrm{res}},\bar{\omega}_{\mathrm{res}})|_{\max}$ for the modes with $n \geqslant 1$ and $s \geqslant 1$ show that if $\beta \to 0$ (that is equivalent to $\bar{q}_z \to \infty$) we have

$$\frac{|E_{zn}(\bar{\rho},\bar{q}_{z,\mathrm{res}},\bar{\omega}_{\mathrm{res}})|_{\max}}{|H_{zn}(\bar{\rho},\bar{q}_{z,\mathrm{res}},\bar{\omega}_{\mathrm{res}})|_{\max}} \propto \sqrt{\frac{\mu(\bar{\omega})}{\varepsilon(\bar{\omega})}}.$$

Since $|\mu(\bar{\omega})| \to \infty$ and $\varepsilon(\bar{\omega})$ remains a finite quantity if $\bar{q}_z \to \infty$ and $\bar{\omega}(\bar{q}_z) \to \bar{\omega}_r$ (i.e., the dispersion curves of bulk-surface waves approach the straight line $\bar{\omega} = \bar{\omega}_r$ asymptotically), we have $|E_{zn}(\bar{\rho},\bar{q}_{z,\mathrm{res}},\bar{\omega}_{\mathrm{res}})|_{\max}/|H_{zn}(\bar{\rho},\bar{q}_{z,\mathrm{res}},\bar{\omega}_{\mathrm{res}})|_{\max} \to \infty$. This explains the fact that at the resonance points $(\bar{q}_{z,\mathrm{res}},\bar{\omega}_{\mathrm{res}})$, if $\bar{q}_{z,\mathrm{res}} > 1$, we have $|E_{zn}(\bar{\rho},\bar{q}_{z,\mathrm{res}},\bar{\omega}_{\mathrm{res}})|_{\max}/|H_{zn}(\bar{\rho},\bar{q}_{z,\mathrm{res}},\bar{\omega}_{\mathrm{res}})|_{\max} > 1$.

Consequently, in the electrodynamic system under study, the tubular electron beam excites coupled bulk-surface

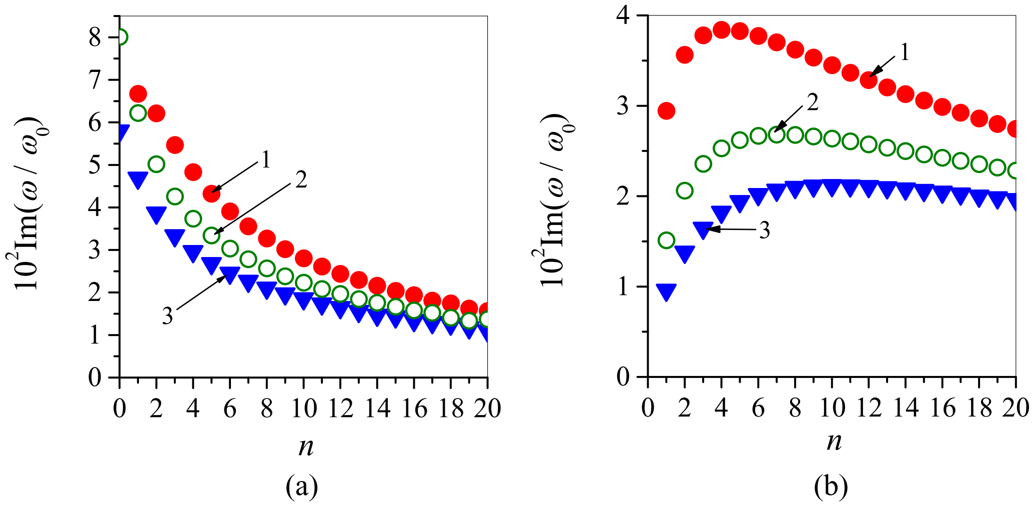

FIG. 8. Instability increment values of an electrodynamic system with the bulk-surface modes corresponding to the low-frequency (*a*) and high-frequency (*b*) branches of the pairs of dispersion dependences for cylinder eigenmodes. In Fig. 8(a), the dependences of the increment values of the E_{0s} and the HE_{ns}^- modes with the radial indices $s = 1, 2, 3$ on the azimuthal index n are labeled by the numbers 1, 2, and 3, respectively. In Fig. 8(b), the numbers 1, 2, and 3 are for the dependences of the increment values of the HE_{ns}^+ modes with $s = 3, 5, 7$ on the azimuthal index n, respectively.

symmetric E_{0s} modes with radial indices $s \geqslant 2$ and hybrid $HE_{ns}^{\pm}$ modes with radial indices $s \geqslant 1$, where the subscripts "–" and "+" refer to the low- and high-frequency branches of the pairs of dispersion dependencies for cylinder eigenmodes, respectively. In doing so, it is supposed that the cylinder is made of the metamaterial, which possesses left-handed properties in the frequency range of interest. In this case, the absolute instability of the aforementioned modes occurs.

Figure 8 shows the increment values $\mathrm{Im}\bar{\omega}$ of excited bulk-surface modes with azimuthal indices in the range $n = 0 \cdots 20$. In Figs. 8(a) and 8(b), these values correspond to the low- and high-frequency branches of the pair of dispersion curves, respectively. Note that in Figs. 3 and 4 the dispersion dependences for the modes with $n = 0, 1$ and $s = 1, 2$ are only shown. The increment values are grouped in accordance with the radial index s of cylinder eigenmodes, which is determined by the order number of the pair of dispersion curves. In Fig. 8(a), the dependences of the increment values of the E_{0s} and HE_{ns}^- modes with the radial indices $s = 1, 2, 3$ on the azimuthal index n are labeled by the numbers 1, 2, and 3, respectively. In Fig. 8(b), the numbers 1, 2, and 3 are for the dependences of the increment values of the HE_{ns}^+ modes with $s = 3, 5, 7$ on the azimuthal index n, respectively.

The analysis of the instability shows that the symmetric bulk-surface $E_{0\,2}$ mode has the maximum increment. In Fig. 8 the increments $\mathrm{Im}\bar{\omega}$ decrease with increasing n because both the value of $|\mu(\bar{\omega}_{\mathrm{res}})|$ and its frequency derivative in the denominator of Eq. (29) increase with frequency. In fact, with increasing n at a fixed value of s the resonant frequencies $\bar{\omega}_{\mathrm{res}}$ tend to the frequency $\bar{\omega}_r$ at which the cylinder permeability increases indefinitely. As shown in Fig. 8(b), the value of azimuthal index n that corresponds to the maximum increment of the HE_{ns}^+ mode increases with radial index s. Therefore, on curve 3 the $HE_{10\,7}^+$ mode has maximum increment. This enables the excitation of the weak decaying whispering gallery modes with large values of azimuthal index n in the electrodynamic system under study.

IV. CONCLUSIONS

The instability of a nonrelativistic tubular electron beam that moves above a dispersive metamaterial of cylindrical configuration has been theoretically examined. It has been assumed that the metamaterial possesses negative permittivity and negative permeability simultaneously over a certain frequency range where it behaves like a LHM. The dispersion equations for eigenmodes of the cylinder and for the coupled modes of the system as well as the instability increments have been derived. The instability is shown to be caused by Cherenkov or anomalous Doppler effects depending on the radial distance between the cylinder and the beam.

The numerical analysis of the dispersion curves of the eigenmodes of the cylinder and the coupled modes excited by the beam in the frequency region where the metamaterial demonstrates the left-handed behavior has been performed. It has been revealed that the parts of the dispersion curves of the bulk-surface waves with anomalous dispersion emerge. The latter implies negative group velocities of corresponding waves and results in the absolute character of the beam instability. It has been found that the resonance behavior of the magnetic permeability of the metamaterial leads to the fact that all bulk-surface waves excited by the beam are the E-type waves for the resonance values of frequencies and wave vectors. The numerical analysis of the dependencies of the instability increments on azimuthal and radial mode indices has been performed. We have shown that the HE_{ns}^+ modes with large radial indices ($s \gg 1$) are the whispering gallery modes for which $n \gg 1$.

Thus this suggests applications of LHMs as delaying media for the generation of bulk-surface waves and eliminates the need for creating artificial feedbacks in slow-wave structures.

[1] R. Kompfner, *The Invention of the Traveling-Wave Tube* (San Francisco Press, San Francisco, 1964).
[2] L. A. Vainshtein and V. A. Solntsev, *Lectures on Ultrahigh-Frequency Electronics* (Sovetskoe Radio, Moskow, 1973) (in Russian).
[3] D. I. Trubetskov and A. E. Hramov, *Lectures on Ultrahigh-Frequency Electronics for Physicists* (PhysMathLitt, Moscow, 2003), Vol. 1 (in Russian).
[4] G. V. Sotnikov, T. C. Marshall, and J. L. Hirshfield, Phys. Rev. Spec. Top.–Accel. Beams **12**, 051301 (2009).
[5] *Encyclopedia of Low-Temperature Plasma*, edited by V. E. Fortov (Science, Moscow, 2000), Vol. 4, (in Russian).
[6] M. V. Kuzelev, A. A. Rukhadze, and P. S. Strelkov, *Plasma Relativistic Microwave Electronics* (Publishing House of the N. E. Bauman Moscow State Technical University, Moscow, 2002) (in Russian).
[7] R. K. Parker, R. H. Abrams, B. G. Danly, and B. Levush, IEEE Trans. Microwave Theory Tech. **50**, 835 (2002).
[8] J. B. Pendry, A. J. Holden, W. J. Stewart, and I. Youngs, Phys. Rev. Lett. **76**, 4773 (1996).
[9] J. B. Pendry, A. J. Holden, D. J. Robbins, and W. J. Stewart, J. Phys.: Condens. Matter **10**, 4785 (1998).
[10] D. R. Smith, W. J. Padilla, D. C. Vier, S. C. Nemat-Nasser, and S. Schultz, Phys. Rev. Lett. **84**, 4184 (2000).
[11] R. A. Shelby, D. R. Smith, S. C. Nemat-Nasser, and S. Schultz, Appl. Phys. Lett. **78**, 489 (2001).
[12] R. A. Shelby, D. R. Smith, and S. Schultz, Science **292**, 77 (2001).
[13] J. T. Huangfu, L. X. Ran, H. S. Chen, X. M. Zhang, K. S. Chen, T. M. Grzegorczyk, and J. A. Kong, Appl. Phys. Lett. **84**, 1537 (2004).
[14] H. S. Chen, L. X. Ran, J. T. Huangfu, X. M. Zhang, and K. S. Chen, Phys. Rev. E **70**, 057605 (2004).
[15] G. Dolling, C. Enkrich, M. Wegener, C. M. Soukoulis, and S. Linden, Opt. Lett. **31**, 1800 (2006).
[16] J. Wang, Z. Xu, B. Du, S. Xia, and J. Wang, J. Appl. Phys. **111**, 044903 (2012).
[17] D. Liu, Z. Xu, N. Ma *et al.*, Appl. Phys. A **106**, 949 (2012).
[18] A. V. Dormidontov, A. Ya. Kirichenko, Yu. F. Lonin, A. G. Ponomarev, Yu. V. Prokopenko, G. V. Sotnikov, V. T. Uvarov, and Yu. F. Filippov, Tech. Phys. Lett. **38**, 85 (2012).
[19] N. S. Ginzburg, V. Y. Zaslavskii, A. M. Malkin, and A. S. Sergeev, Tech. Phys. **57**, 1692 (2012).
[20] N. S. Ginzburg, V. Y. Zaslavskii, A. M. Malkin, and A. S. Sergeev, Tech. Phys. **58**, 267 (2013).
[21] K. V. Galaydych, Yu. F. Lonin, A. G. Ponomarev, Yu. V. Prokopenko, and G. V. Sotnikov, Probl. At. Sci. Technol., Ser.: Plasma Phys. **6**, 123 (2010).
[22] K. V. Galaydych, Yu. F. Lonin, A. G. Ponomarev, Yu. V. Prokopenko, and G. V. Sotnikov, Probl. At. Sci. Technol., Ser.: Plasma Phys. **6**, 158 (2012).
[23] V. P. Silin and A. A. Rukhadze, *Electromagnetic Properties of Plasma and Plasma-Like Media* (Gosatomizdat, Moscow, 1961) (in Russian).
[24] G. Bekefi, *Radiation Processes in Plasmas* (Wiley, New York, 1966).
[25] L. D. Landau and E. M. Lifshits, *Electrodynamics of Continuous Media* (Science, Moscow, 1982) (in Russian).
[26] A. V. Dormidontov, Yu. V. Prokopenko, S. I. Khankina, and V. M. Ylakovenko, Telecommun. Radio Eng. (Engl. Transl.) **73**, 1165 (2014).
[27] A. V. Dormidontov, Yu. V. Prokopenko, S. I. Khankina, and V. M. Yakovenko, Telecommun. Radio Eng. (Engl. Trans.) **75**, 507 (2016).
[28] A. V. Dormidontov, Yu. V. Prokopenko, and V. M. Yakovenko, Telecommun. Radio Eng. (Engl. Transl.) **75**, 201 (2016).
[29] A. V. Dormidontov, Yu. V. Prokopenko, S. I. Khankina, and V. M. Yakovenko, Tech. Phys. **60**, 1069 (2015).
[30] Yu. O. Averkov, Yu. V. Prokopenko, and V. M. Yakovenko, J. Exp. Theor. Phys. **121**, 699 (2015).
[31] Yu. O. Averkov, Yu. V. Prokopenko, and V. M. Yakovenko, Telecommun. Radio Eng. (Engl. Transl.) **75**, 1467 (2016).
[32] V. E. Pafomov, Zh. Eksp. Teor. Fiz. **36**, 1853 (1959) (in Russian).
[33] V. G. Veselago, Usp. Fiz. Nauk **92**, 517 (1967) [Sov. Phys. Usp. **10**, 509 (1968)].
[34] Y. Song, J. Ta, H. Li, and X. Z. Wang, J. Appl. Phys. **106**, 063119 (2009).
[35] D. Wang, L. Ran, H. Chen, and M. Mu, Appl. Phys. Lett. **91**, 164101 (2007).
[36] A. L. Pokrovsky and A. L. Efros, Phys. Rev. Lett. **89**, 093901 (2002).
[37] T. Koschny, M. Kafesaki, E. N. Economou, and C. M. Soukoulis, Phys. Rev. Lett. **93**, 107402 (2004).
[38] V. M. Agranovich, Y. R. Shen, R. H. Baughman, and A. A. Zakhidov, Phys. Rev. B **69**, 165112 (2004).
[39] Yu. O. Averkov and V. M. Yakovenko, Phys. Rev. B **72**, 205110 (2005).
[40] Yu. P. Bliokh, S. Savel'ev, and F. Nori, Phys. Rev. Lett. **100**, 244803 (2008).
[41] Yu. O. Averkov, A. V. Kats, and V. M. Yakovenko, Phys. Rev. B **79**, 193402 (2009).
[42] S. N. Galyamin and A. V. Tyukhtin, Phys. Rev. B **81**, 235134 (2010).
[43] X. S. Rao and C. K. Ong, Phys. Rev. B **68**, 113103 (2003).
[44] Y. Dong and X. Zhang, J. Appl. Phys. **105**, 054105 (2009).
[45] Zhong-hao Sa, Yin Poo, Rui-xin Wu, and Chao Xiao, Appl. Phys. A **117**, 427 (2014).
[46] S. Antipov, W. Liu, W. Gai, J. G. Power, and L. Spentzouris, AIP Conf. Proc. **877**, 815 (2006).
[47] G. V. Sotnikov and T. C. Marshall, Phys. Rev. Spec. Top.–Accel. Beams **14**, 031302 (2011).
[48] *Handbook of Special Functions, with Formulas, Graphs and Tables*, edited by M. Abramovitsa and I. Stigan (Science, Moscow, 1979) (in Russian).
[49] A. Ya. Kirichenko, Yu. V. Prokopenko, Yu. F. Filippov, and N. T. Cherpak, *Quasi-Optical Solid-State Resonators* (Naukova Dumka, Kiev, 2008) (in Russian).
[50] M. V. Nezlin, Usp. Fiz. Nauk **120**, 481 (1976) [Sov. Phys. Usp. **19**, 946 (1976)].
[51] A. I. Akhiezer, I. A. Akhiezer, R. V. Polovin, A. G. Sitenko, and K. N. Stepanov, *Plasma Electrodynamics* (Pergamon Press, New York, 1975).
[52] R. Ruppin, Phys. Lett. A **277**, 61 (2000).
[53] J. A. Nelder and R. Mead, Comput. J. **7**, 308 (1965).

[54] Ya. B. Fineberg and V. D. Shapiro, To the nonlinear theory of interaction between relativistic beam and plasma, In *Interaction of Charged Particles Beams with Plasma* (Publishing House of the Academy of Sciences of Ukrainian SSR, Kiev, 1965) (in Russian).

[55] P. A. Sturrock, Proc. R. Soc. A **242**, 277 (1957).

[56] G. A. Korn and T. M. Korn, *Mathematical Handbook for Scientists and Engineers. Definitions, Theorems, and Formulas for Reference and Review* (Dover Publications, Inc., Mineola, NY, 1968).

[57] L. A. Vaynshteyn, *Electromagnetic Waves* (Sovetskoe Radio, Moscow, 1957) (in Russian).